Molecular dynamics studies for the new refrigerant R152a with simple model potentials

by CARLOS VEGA†, BERTHOLD SAAGER
and JOHANN FISCHER

Institut für Thermo- und Fluiddynamik, Ruhr-Universität,
D-4630 Bochum 1, F.R. Germany

The new refrigerant R152a (CH_3–CHF_2) is modelled as a fluid of homonuclear two-centre Lennard-Jones molecules with a point dipole along the axis. This 2CLJD potential has four parameters which were determined by using results of previous and new molecular dynamics simulations for 2CLJD molecules of elongation $L^* = 0.505$ and different reduced dipole moments μ^*. For each of these dipole moments zero pressure liquid densities at two temperatures were taken to determine the Lennard-Jones parameters ε and σ from a fit to experimental saturated liquid densities. A subsequent comparison of calculated second virial coefficients with experimental values led to the conclusion that $\mu^{*2} = 8$ in combination with $\varepsilon/k = 119.0$ K and $\sigma = 3.845$ Å is a reasonable choice. Further simulations with those parameters, all performed with vectorized codes on a CYBER 205, gave reasonable predictions of the thermodynamic properties. As the reduced dipole moment $\mu^{*2} = 8$ corresponds to 2.73 D compared to the experimental value of 2.27 D, the effect of rotating the dipole vector out of the molecular axis was also investigated. It is found that for a dipole vector forming some angle with the molecular axis a smaller value of the dipole moment is required to produce similar thermodynamic properties as for the case when the dipole is along the axis. Spherical harmonic expansion coefficients $g_{ll'm}$ of the pair correlation function are given for the model with and without the dipole and also for three different orientations of the dipole vector with respect to the molecular axis.

1. Introduction

For over 20 years it has been conjectured that some of the halocarbons which are used extensively as spray driving and foam blowing gases, as solvents and as refrigerants, may rise into the upper atmosphere without being decomposed. These conjectures gained substance when it was realized some years ago that there is a depletion of the ozone layer that could be attributed to the chlorine contained in fully halogenated chlorofluorocarbons. Possible substitutes for the common refrigerants could be halocarbons which contain as little chlorine as possible but some hydrogen atoms which facilitate their decomposition. Candidates of interest are R152a (CH_3–CHF_2), R142b (CH_3–$CClF_2$) and R134a (CH_2F–CF_3) which are all derivatives of ethane with strong dipole moments.

Presently, most experimental data seems to be available for R152a from measurements performed in Japan [1–5], in the Soviet Union [6], in France [7], and

† Permanent address: Departmento de Quimica Fisica, Facultad de Ciencias Quimicas, Universidad Complutense, E-28040 Madrid, Spain.

recently also in Germany [8]. Unfortunately the original data for the correlation of Mears [9] which were deposited at the American Documentation Institute seem to be not easily available at present.

Motivated by this environmental challenge we thought it interesting to perform statistical mechanical studies for these new refrigerants with the main emphasis on obtaining an understanding of their thermodynamic behaviour. Because of the favourable experimental situation we decided to start with R152a.

The main problem with such a study is the choice of the model potential and of the potential parameters. A sophisticated potential will be able to fit thermodynamic data over a large range of the phase diagram, but it is also clear that the search for the potential parameters becomes a very difficult task when their number is increased. In addition there is still the technical problem that with increasing complexity of the potential model the computer time required for simulations also increases. In this work we decided to choose a simple model that includes the nonspherical shape and the dipole moment of the CH_3-CHF_2 molecule. The simplest conceivable model then is a homonuclear two-centre Lennard-Jones potential with a dipole along the molecular axis (2CLJD).

The question still remains as to how the potential parameters are to be determined. In previous work [10–13] potential parameters for n-centre Lennard-Jones (nCLJ) molecules were determined by fitting the saturation curve obtained from perturbation theory to the experimental data. Recently, it was shown using computer simulations that with the parameters determined in this way, thermodynamic properties at other state points can be predicted nearly within experimental accuracy for methane [14], ethane [15–17], oxygen [17] and ethylene [17]. After a slight change in the size parameter the predictions for propane were also excellent [18]. Unfortunately, this method can not be applied for the 2CLJD-model as we have not yet succeeded in extending perturbation theory to polar molecules [19]. Hence, in the present study we fixed the molecular elongation from the very beginning and determined the other parameters by using the method of zero-pressure-liquid-densities [20] which was supplemented by fits to the second virial coefficient. Details of this procedure are described in § 2.

Once the potential parameters are determined, simulations are performed for a variety of state points and the resulting thermodynamic properties are compared with available experimental data in § 3. In § 4 the changes in the structural and thermodynamic properties caused by switching on the dipole along the axis are considered.

For CH_3-CHF_2 molecule we know that the dipole vector should not be parallel to the molecular axis. In § 5 we investigate the effect of rotating the dipole vector out of this axis. Second virial coefficients, thermodynamic properties of the dense fluid as well as some structural information are presented.

Section 6 contains our conclusions.

2. Determination of the 2CLJD potential parameters

The potential used in the first part of the present studies is a homonuclear two-centre Lennard-Jones potential plus a point dipole located in the centre of the molecule with the dipole vector along the molecular axis. Such a model has four parameters: the two Lennard-Jones site–site parameters ε and σ, the distance l between the Lennard-Jones (LJ) sites given most conveniently by the reduced

Table 1. Raw simulation data used for the determination of the zero pressure densities at two temperatures and different reduced dipole moments μ^* (all for 2CLJD with $L^* = 0.505$).

μ^{*2}	kT/ε	$\rho\sigma^3$	$p\sigma^3/\varepsilon$
2	2·155	0·466	0·13†
		0·548	2·70†
		0·629	9·49†
	1·539	0·548	−0·17†
		0·629	5·05†
4	2·155	0·466	−0·21†
		0·548	2·20†
		0·629	8·72†
	1·539	0·548	−0·67†
		0·629	4·42†
8	2·155	0·466	−0·97†
		0·466	−0·94‡
		0·505	−0·24‡
		0·515	−0·04‡
		0·525	0·29‡
		0·548	1·09†
		0·629	7·21†
	1·539	0·548	−1·79†
		0·590	−0·10‡
		0·592	0·05‡
		0·600	0·58‡
		0·629	2·77†

† From [21] (500 particles, 2000 equilibration and 10 000 production time steps).
‡ Results from this work (256 particles, 2000 equilibration and 5000 production time steps).

quantity $L^* = l/\sigma$ and finally the dipole moment μ given in reduced units as $\mu^* = \mu/(\varepsilon\sigma^3)^{1/2}$.

We decided to fix the elongation L^* at 0·505 from the very beginning. One reason for that choice was that simulation results were available for 2CLJD molecules of that elongation at 28 state points with 5 different values of μ^* at each state point [21]. More important, however, are some physical arguments. Previously, for ethane the 2CLJ parameters $\sigma = 3.5$ Å and $L^* = 0.67$ [10] and for propane the 3CLJ parameters $\sigma = 3.54$ Å and $L^* = 0.61$ [12] were found. It is thought that the large elongation for ethane accounts in some sense for the quadrupole which was not considered explicitly in the model. Now, if we assume for CH_3–CHF_2 the LJ sites are at the same distance as in propane but consider the molecule as a whole to be bigger than two methyl groups, then an elongation of about 0·5 seems to be a reasonable choice for a simple model.

Once L^* was fixed, the other three parameters were determined in the following manner. For some values of the reduced dipole moment μ^* the reduced zero-pressure-densities $\rho_0\sigma^3$ of the liquid were determined by molecular dynamics simulations at two reduced temperatures kT/ε. Then, by following Singer *et al.* [20] and using the experimentally known saturated liquid densities [3] as approximations for the zero pressure densities one can determine for each value of μ^* a pair of ε- and

Table 2.   Potential parameters ε and σ for 2CLJD ($L^* = 0.505$)-fluids obtained by fitting the
zero pressure densities from simulations to the experimental saturated liquid densities
from simulations to the experimental saturated liquid densities of R152a [3] for three
different values of the reduced dipole moment μ^*. The table also contains the corre-
sponding dipole moments μ in Debye.

Parameter set	μ^{*2}	$(\varepsilon/k)/K$	$\sigma/\text{Å}$	μ/D
PS1	2	134·0	3·802	1·42
PS2	4	130·8	3·810	2·00
PS3	8	119·0	3·845	2·73

σ-values. The choice of the value of μ^* is then made by calculating the second virial
coefficients and comparing them with the experimental values [5, 8].

Details of the molecular dynamics simulations and of the second virial coeffi-
cient calculations are given in the Appendix.

In the actual procedure the reduced dipole moments, $\mu^{*2} = 2$, 4, and 8, and the
temperatures, $kT/\varepsilon = 1.539$ and 2·155, were used. For these values simulation
results were already available at several reduced densities [21]. For $\mu^{*2} = 8$ addi-
tional simulations were performed for other densities at both temperatures. The
previous and present simulation results are all compiled in table 1. As a first step,
zero-pressure-densities were determined by interpolation or extrapolation. Next, in
order to obtain values of ε and σ for each value of μ^{*2}, an iteration procedure was
applied. We chose a trial value for ε and converted the two reduced temperatures
into real temperatures. Then at each of these two temperatures the zero pressure
density was fitted to the experimental saturated liquid density [3] which gave two
values of σ. If the two values of σ were different, we chose an other trial value of ε
and the procedure was repeated till the two values of σ became identical. The
resulting parameter sets, called PS1, PS2, and PS3 are given in table 2. This table
also contains the corresponding dipole moments in Debye‡ and we should note that
the experimental dipole moment for R152a is 2·27 D [22].

In table 2 we observe that the site–site energy parameter ε is strongly correlated
to the value of the dipole moment. If the dipole moment increases, the attractive
dispersion energy has to decrease so that the total cohesion energy keeps the
volume of the system unchanged. The variation of σ, whilst not so pronounced,
seems to be a consequence of the change in ε. With decreasing ε the effective hard
core of the molecule would also decrease and that is compensated by an increase
in σ.

The choice of the best of the three values of μ^* used so far is then made by
calculating the second virial coefficients with the parameter sets PS1, PS2, and PS3
determined above and comparing with experimental data. The results are shown in
table 3.

From table 3 we learn that PS3 with $\mu^{*2} = 8$ or $\mu = 2.73$ D shows the best
agreement with the experimental second virial coefficients and it is this parameter
set that will be used in the following sections. It is interesting to note that according
to table 3 one would expect an even higher dipole moment than $\mu^{*2} = 8$ to yield
better agreement with the experimental results, whilst on the other hand the un-
reduced PS3 dipole moment of 2·73 D is already considerably higher than the

‡ 1 Debye = 3.3357×10^{-30} C m.

Table 3. Second virial coefficients for 2CLJD ($L^* = 0.505$) potentials with the parameter sets PS1, PS2, and PS3 from table 2 in comparison with experimental data of R152a [5, 8].

	$B \times 10^6/\text{m}^3\,\text{mol}^{-1}$			
T/K	PS1	PS2	PS3	Exp
233·15	−455	−558	−935	−1109†
253·15	−388	−461	−747	−844†
273·15	−334	−396	−612	−671†
290·00	−297	−349	−526	−541‡
296·15	−286	−330	−500	−534†
310·00	−261	−303	−447	−446‡
330·00	−230	−266	−384	−382‡
350·00	−205	−235	−333	−315‡
370·00	−183	−209	−292	−267‡
390·00	−164	−186	−258	−246‡
410·00	−148	−167	−228	−220‡
420·00	−140	−158	−215	−209‡

† [8]. ‡ [5].

experimental value 2·27 D. One explanation could be that dipole induced-dipole interactions not considered here can be compensated for by an effective higher dipole moment [23]. We believe, however, that the difference is too large to be explained only by induction effects and conjecture that the angle of the dipole vector with the molecular axis as it actually occurs in R152a could be another reason for the discrepancy. We address this question again in § 5.

3. Thermodynamic properties of the 2CLJD-PS3 fluid

With the 2CLJD-model in combination with the parameter set PS3 determined in the last section we performed several molecular dynamics simulations in order to obtain thermodynamic properties to be compared with the experimental results of R152a.

The one set of properties we are comparing with is the $p\rho T$-data. In passing, we note that the critical quantities of R152a are $T_c = 386·44\,\text{K}$, $\rho_c = 5·57\,\text{mol/dm}^3$ and $p_c = 4·52\,\text{MPa}$ [2]. Geller *et al.* [6] measured data on 14 liquid isochores ranging from 18 down to 10 mol/dm^3. From those we chose 4 isochores including the highest and the lowest density and on each of them the highest and the lowest temperature. Iso and Uematsu [1] gave data on isotherms ranging from the subcritical liquid branch at 320 K up to the supercritical isotherm at 400 K. Here we chose the lowest and the highest isotherm and the lowest and highest density on each of them. All the calculated pressures are compiled in table 4 which also contains the configurational internal energies.

In order to judge the quality of the predictions we should begin by discussing the uncertainties in the simulated pressures. We did not perform systematic studies to evaluate these errors but we found previously [14] for spherical Lennard-Jones molecules that the uncertainty in $p\sigma^3/\varepsilon$ increases from 0·005 at about the critical density ρ_c to 0·100 at about 3·5 ρ_c. We believe that for nonspherical molecules the uncertainty will be somewhat larger but of the same order of magnitude. Since for

Table 4. Pressures and configurational internal energies from MD simulations for 4 iso-
chores and 2 isotherms. The pressures are compared to experimental results [1, 6].

T/K	$\rho/\text{mol dm}^{-3}$	p/MPa Exp	p/MPa§ Sim	$U_{\text{conf}}/\text{kJ mol}^{-1}$§ Sim
158·81	17·970	0·84†	7·38	−22·25
181·90	17·921	48·35†	41·22	−21·77
210·83	16·507	1·52†	0·85	−19·91
242·34	16·455	44·82†	38·02	−19·32
302·16	13·514	1·54†	−0·90	−15·65
364·87	13·450	42·02†	37·01	−14·89
371·45	9·859	3·98†	2·34	−11·37
470·18	9·809	29·82†	26·12	−10·55
320	12·811	1·50‡	1·21	−14·71
320	13·368	10·00‡	10·35	−15·25
400	3·532	5·14‡	5·20	−5·18
400	9·544	10·00‡	8·12	−10·85

† From [6].
‡ From [1].
§ MD from this work (256 particles, 8000 equilibration and 12 000 production time steps).

our model $p\sigma^3/\varepsilon = 1$ corresponds to about 30 MPa, we estimate the uncertainty in the pressure at the highest density to be about 3 MPa.

Comparison with the data of Geller *et al.* [6] shows differences in the pressure up to 7 MPa which at the first sight seems to be rather large. But we should keep in mind that the isochores there are rather steep and only a small change in the size of the molecular core has a dramatic effect for the pressure. On the other hand we know from recent experiments on R22 in our laboratory [24] that the values assigned by Geller *et al.* [6] to the density are uncertain up to 0·5 per cent which at the highest densities corresponds to an uncertainty of 6 MPa. We must, however, admit that in spite of the combined experimental and simulation uncertainties there seems to be a systematic discrepancy as the experimental isotherms are always steeper than the calculated ones which indicates a certain deficiency of our model.

We observe quite good agreements at 320 K with the data of Iso and Uematsu [1] but a somewhat low pressure at 400 K for the higher density.

A property of considerable practical interest is the enthalpy of vapourization. For this property and the dew density, experimental values do not yet exist. So far, both these quantities have been calculated from a Redlich–Kwong–Soave (RKS) equation [3]. Nevertheless, we thought it would be interesting to compare also with caloric quantities obtained from such correlations. We did not apply here recently developed methods for the determination of phase equilibria [25–27] from computer simulations and hence do not know the vapour liquid equilibrium for our model. Hence, we decided to consider the liquid at the experimentally known bubble density and the vapour at the dew density obtained from the RKS-equation [3] and to calculate the energy difference between these two state points which is the energy of vaporization. These calculations were performed at 302·16 K and 371·45 K for which liquid state results are already given in table 4. As these state points are not just at the saturation curve but somewhat shifted into the homogeneous liquid we determined $(\partial U/\partial \rho)_T$ on the two isotherms $T = 320$ K and 400 K and from table 4 obtained the values −0·97 and −0·94 kJ dm^3/mol^2, respectively.

Table 5. Energies of vaporization U_{vap} from simulations in comparison with those from the RKS-equation [3]. Given are also the dew densities ρ'' from the RKS-equation [3], experimental bubble densities ρ' [2, 3] and vapour pressures $p(\rho'')$ obtained from gas phase simulations at the RKS dew densities.

T/K	$\rho''/\mathrm{mol\,dm^{-3}}$ RKS	$\rho'/\mathrm{mol\,dm^{-3}}$ Exp	$U_{vap}/\mathrm{kJ\,mol^{-1}}$ RKS	$U_{vap}/\mathrm{kJ\,mol^{-1}}$ Sim	p_σ/MPa Exp	$p(\rho'')/\mathrm{MPa}$ Sim
302·16	0·312	13·456†	16·25	15·00	0·67	0·69
371·45	2·065	9·550‡	8·23	7·94	3·39	3·76

† From [3].
‡ From [2].

An average value then was used to correct for the difference of the configurational internal energy between the simulated state point and the saturated liquid density. This correction is $0.06\,\mathrm{kJ\,mol^{-1}}$ at the lower and $0.30\,\mathrm{kJ\,mol^{-1}}$ at the higher temperature. On the gas side, additional simulations were performed just at the dew densities obtained from the RKS-equation [3].

The results for the energies of vaporization are compared in table 5 with those from the RKS-equation [3]. We see that our results are always smaller, by about 3 per cent at the higher temperature and by about 8 per cent at the lower temperature.

From the gas phase simulations at the RKS dew densities we also obtain pressures, which are compared in table 5 with the experimental vapour pressures. The agreement which is nearly within the accuracy of the simulations can be termed reasonable.
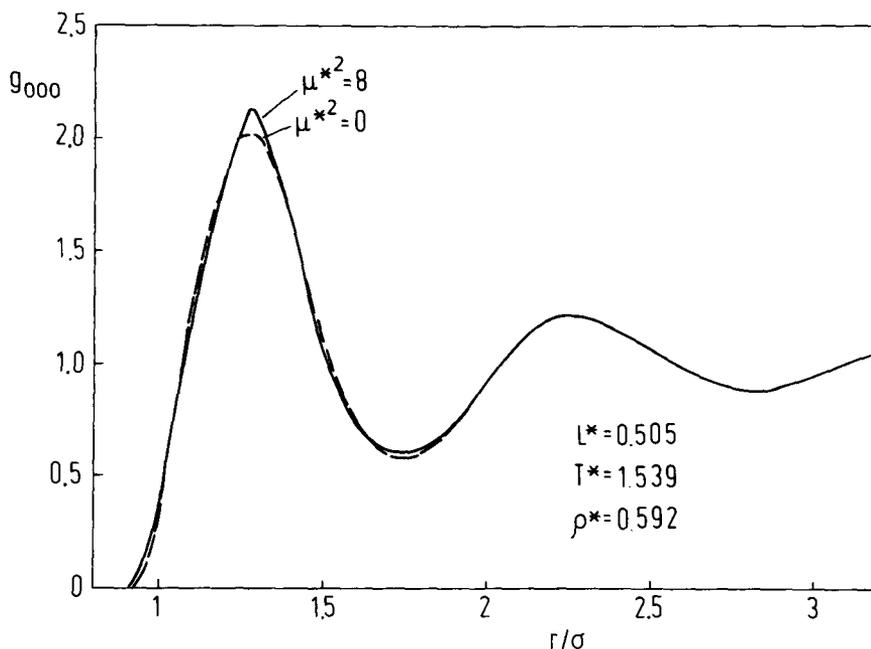
Figure 1. The angle averaged centre–centre pair correlation functions g_{000} of a 2CLJ and a 2CLJD (dipole along the axis) fluid. The latter has a reduced squared dipole moment $\mu^{*2} = 8$, the site–site interactions are the same in both cases ($L^* = 0.505$, $\varepsilon/k = 119.0\,\mathrm{K}$, and $\sigma = 3.845\,\text{Å}$).

4.   Effects of the dipole along the axis on structure and thermodynamics

It is interesting to investigate the effect of the dipole on structure and thermo-dynamics. For that purpose we compare structural results obtained for a 2CLJ and a 2CLJD (dipole along the axis) fluid with both the same site–site parameters of PS3 ($L^* = 0.505$, $\varepsilon/k = 119.0\,\mathrm{K}$, $\sigma = 3.845\,\text{Å}$. The reduced dipole moment of the 2CLJD interaction is also that of PS3, namely $\mu^{*2} = 8$. The thermodynamic results will also be compared and the dipole–dipole contribution to the energy analysed.

One possibility for analysing angle-dependent pair correlation functions of linear molecules is their expansion in spherical harmonics [28] in the intermolecular frame

$$g(r, \omega_1, \omega_2) = 4\pi \sum_{ll'm} g_{ll'm}(r) Y_{lm}(\omega_1) Y_{l'-m}(\omega_2). \tag{1}$$

The structural results are presented in figure 1 to 3.

Here and in the following, reduced quantities $T^* = kT/\varepsilon$, $\rho^* = \rho\sigma^3$ and $U^* = U/N\varepsilon$ are used; the stars will be omitted if there is no ambiguity.

Figure 1 shows the angle averaged centre–centre pair correlation functions g_{000}. It is seen that switching on a rather strong dipole does not change this function much. The major difference is in the first peak which is higher for the 2CLJD-fluid. The effect of the dipole in that respect, however, is smaller than that of a quadrupole [19]. Figure 2 shows the next even expansion coefficients, the functions g_{200}. Here again, and also for g_{220} which is not shown here, the effect of the dipole is small which confirms previous findings of Steinhauser [29]. The difference between the dipolar and the non-dipolar fluid, however, is in the odd coefficients which are identically zero for the homonuclear 2CLJ molecules. For the 2CLJD-fluid, the first coefficients g_{110} and g_{111}, which are also of direct importance for thermodynamic properties are given in figure 3.
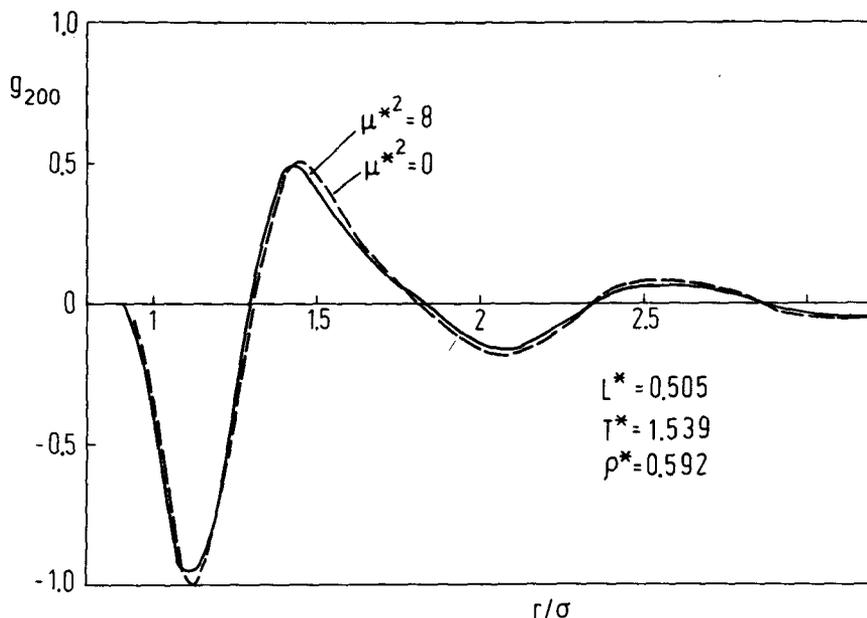
Figure 2.   The spherical harmonic expansion coefficients g_{200} of the pair correlation func-tions of a 2CLJ and a 2CLJD (dipole along the axis) fluid. Molecular interaction and state parameters are the same as in figure 1.
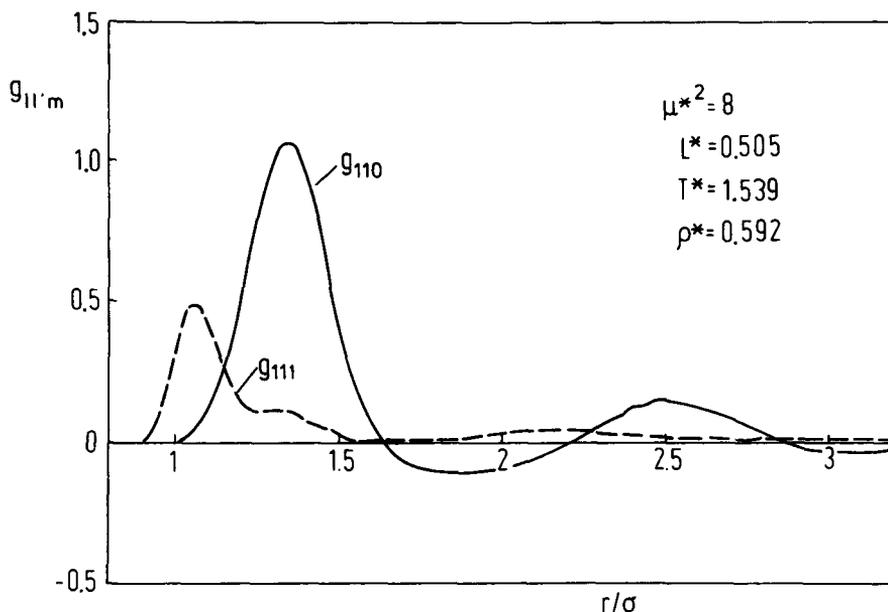
Figure 3. The spherical harmonic expansion coefficients g_{110} and g_{111} of the pair correlation function of the 2CLJD (dipole along the axis) fluid with the same molecular interaction and state parameters as in figure 1.

We separated the contributions due to the dipole–dipole interactions and those due to the 2CLJ–2CLJ-interaction for the 2CLJD-fluid and compared the latter with the properties for the 2CLJ-fluid. The results are displayed in table 6. Firstly, we note that the 2CLJ–2CLJ-contribution to the internal energy of the 2CLJD-fluid is only slightly more positive than the internal energy of the 2CLJ-fluid as was found previously for the quadrupolar case [19]. This behaviour might have been conjectured from the similarity of the even coefficients $g_{ll'm}$ for the 2CLJ and the 2CLJD-fluid. For the pressure, however, the contribution of the 2CLJ-interaction in the 2CLJD-fluid is considerably higher than the pressure of the 2CLJ-fluid. This reflects the well-known fact that the pressure in general is more sensitive to changes in the structure than the energy. The lower pressure of the 2CLJ-fluid may be partly due to the slightly smaller first peak in g_{000}.

The total dipole contribution $U_{DD,\,total}$ to the internal energy consists of the directly counted dipole–dipole interaction U_{DD} and the contribution U_{rf} from the reaction field which are separately listed in table 6. The energy U_{DD} can be analysed as the dipole–dipole potential can be expressed as a sum of three spherical harmonics

$$u_{DD} = -\frac{\mu^2}{3r^3}\,4\pi[2Y_{10}(\omega_1)Y_{10}(\omega_2) + Y_{1-1}(\omega_1)Y_{11}(\omega_2) + Y_{11}(\omega_1)Y_{1-1}(\omega_2)] \qquad (2)$$

Hence, the dipolar energy U_{DD} can also be written as a sum of the two terms

$$U_{DD}^{110} = -\frac{4\pi\rho\mu^2}{3}\int_0^\infty r^{-1}g_{110}(r)\,dr, \qquad (3)$$

Table 6. Contributions to the thermodynamic properties of a 2CLJD-fluid and comparison with a 2CLJ-fluid. Given are the contributions of the 2CLJ–2CLJ-interaction and of the dipole–dipole-interaction to the internal energy and the pressure as well as the total quantities. For the dipolar energy again different contributions are given: the expansion terms U_{DD}^{110}, U_{DD}^{111}, their sum as well as the directly calculated quantity U_{DD} without reaction field contribution (rf), the reaction field energy, and the total dipole–dipole energy. The potential parameters are $L^* = 0.505$, $\varepsilon/k = 119.0$ K, $\sigma = 3.845$ Å for the 2CLJ and the 2CLJD molecules and $\mu^{*2} = 8$ for the latter. The state point is $kT/\varepsilon = 1.539$ and $\rho\sigma^3 = 0.592$. Reduced energies $U/N\varepsilon$ and pressures $p\sigma^3/\varepsilon$ are given.

	2CLJD	2CLJ
$U_{2CLJ-2CLJ}$	-14.65	-15.03
U_{DD}^{110}	-4.40	—
U_{DD}^{111}	-2.12	—
$U_{DD}^{110} + U_{DD}^{111}$	-6.56	—
U_{DD}	-6.65	—
U_{rf}	-0.10	—
$U_{DD, total}$	-6.75	—
U_{total}	-21.40	-15.03
$p_{2CLJ-2CLJ}$†	4.05	2.44
$p_{DD, total}$	-4.00	—
p_{total}	0.05	2.44

† Includes the ideal contribution to the pressure.

$$U_{DD}^{111} = -\frac{4\pi\rho\mu^2}{3} \int_0^\infty r^{-1} g_{111}(r)\, dr. \tag{4}$$

Both these contributions are also contained in table 6 and we see that their sum is in reasonable agreement with the directly calculated U_{DD}.

5. Effects of rotating the dipole out of the axis

From a physical point of view the 2CLJD/PS3 model we are using to describe R152a is not completely satisfactory because the dipole lies along the axis and its magnitude of 2.73 D is considerably larger than the experimental value of 2.27 D. Hence, it is interesting to study the effects of rotating the dipole out of the axis. While the agle α which the dipole vector forms with the molecular axis represented by the C–C bond is not known, we estimated it to be about 54° using ideas of Gibbs and Smyth [30]. Here, we chose $\alpha = 45°$ and in order to gain further insight we also consider $\alpha = 90°$, both in comparison with $\alpha = 0°$. The other parameters, namely L^*, ε, σ, and μ^{*2} remain unchanged.

For the three values $\alpha = 0°$, 45°, and 90° we performed molecular dynamics simulations in the dense fluid at two state points, $T^* = 1.539$, $\rho^* = 0.592$, and $T^* = 2.1546$, $\rho^* = 0.515$. In all cases we calculated the total energies and pressures as well as their contributions from the 2CLJ–2CLJ and from the dipole–dipole interactions. As the qualitative behaviour is the same for both state points we show the results only for the latter in table 7. We learn that rotating the dipole out of the axis decreases the energy as well as the pressure. We also note that the changes in going from $\alpha = 0°$ to $\alpha = 45°$ are about half of those in going from $\alpha = 45°$ to $\alpha = 90°$. This decrease in the pressure and the energy is just what we were looking for because it means that rotating the dipole out of the axis acts in the same sense as

Table 7. Contribution to the thermodynamic properties of two-centre Lennard-Jones plus dipole fluids with different angles α between the dipole vector and the molecular axis. Given are the contributions of the 2CLJ–2CLJ-interaction and of the dipole–dipole interaction to the internal energy and the pressure as well as the total quantities. The potential parameters are $L^* = 0.505$, $\varepsilon/k = 119.0$ K, $\sigma = 3.845$ Å and $\mu^{*2} = 8$, the state point is $kT/\varepsilon = 2.1546$ and $\rho\sigma^3 = 0.515$. Reduced energies $U/N\varepsilon$ and pressures $p\sigma^3/\varepsilon$ are given.

	$\alpha = 0°$	$\alpha = 45°$	$\alpha = 90°$
$U_{2CLJ–2CLJ}$	−12·32	−12·18	−11·80
$U_{DD, total}$	−5·65	−8·05	−12·14
U_{total}	−17·97	−20·23	−23·95
$P_{2CLJ–2CLJ}$†	2·80	3·46	4·82
$P_{DD, total}$	−2·91	−4·15	−6·25
P_{total}	−0·11	−0·69	−1·44

† Includes the ideal contribution to the pressure.

increasing its magnitude. This means that modelling R152a with a dipole vector forming a nonzero angle α with the axis would allow a smaller dipole moment than 2·73 D.

We also calculated second virial coefficients for all three values of α which are displayed in table 8. These results confirm that rotating the dipole out of the axis acts in the same sense as increasing its magnitude.

Again we were also interested in structural properties. As we are dealing now with nonlinear molecules we had to use the expansion of the pair correlation function in Wigner rotation matrices [31] which is

$$g(r, \Omega_1, \Omega_2) = 4\pi \sum_{\substack{ll'm \\ nn'}} \frac{\sqrt{[(2l + 1)(2l' + 1)]}}{4\pi} \hat{g}_{ll'm}^{nn'}(r) \cdot D_{mn}^{l*}(\Omega_1) D_{mn'}^{l'*}(\Omega_2) \tag{5}$$

where Ω_i stands for the Euler angles $(\Phi_i, \Theta_i, \chi_i)$ and D_{mn}^l denotes the rotation matrix. For linear molecules, equation (5) reduces to equation (1) with

$$g_{ll'm}(r) = \hat{g}_{ll'm}^{00}(r). \tag{6}$$

Table 8. Second virial coefficients of two-centre Lennard-Jones plus dipole fluids with different angles α between the dipole vector and the molecular axis. The potential parameters are $L^* = 0.505$, $\varepsilon/k = 119.0$ K, $\sigma = 3.845$ Å, and $\mu^{*2} = 8$. The values are given in cm^3/mol.

T/K	$\alpha = 0°$	$\alpha = 45°$	$\alpha = 90°$
233·15	−935	−1297	−2535
273·15	−612	−782	−1216
290	−526	−657	−962
310	−447	−546	−757
330	−384	−462	−614
350	−333	−396	−510
370	−292	−343	−431
390	−258	−300	−370
410	−228	−264	−321
420	−215	−249	−300
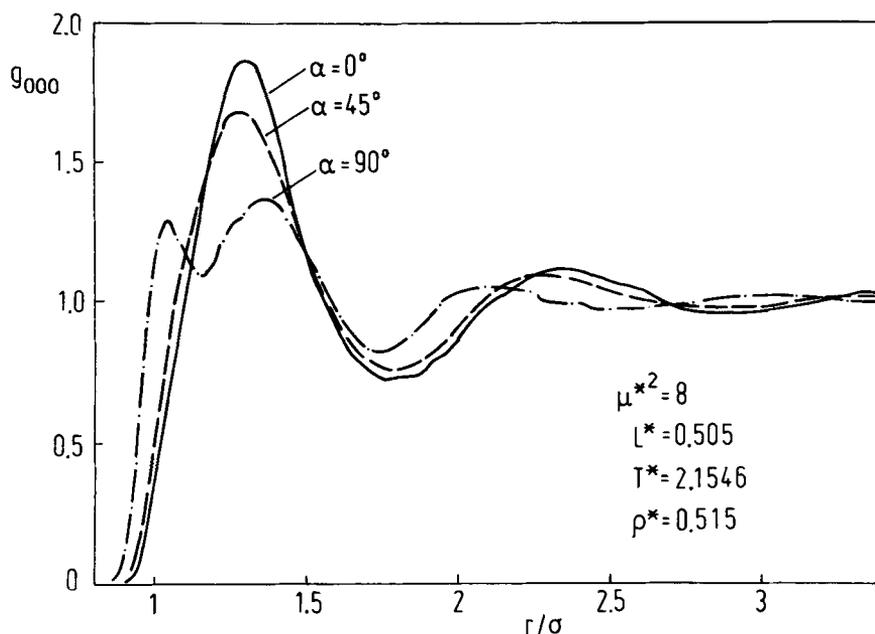
Figure 4. The angle averaged centre–centre pair correlation functions g_{000} of the two-centre Lennard-Jones plus dipole fluids for different angles α between the dipole vector and the molecular axis.

Results for $\hat{g}_{000}^{00}$, $\hat{g}_{110}^{00}$, and $\hat{g}_{200}^{00}$ for all three values of α are shown in figure 4 to 6. For abbreviation, we use there and in the following simply the notation g_{000}, g_{110}, and g_{200}.

The most striking feature in the structure is seen in the angle-averaged centre–
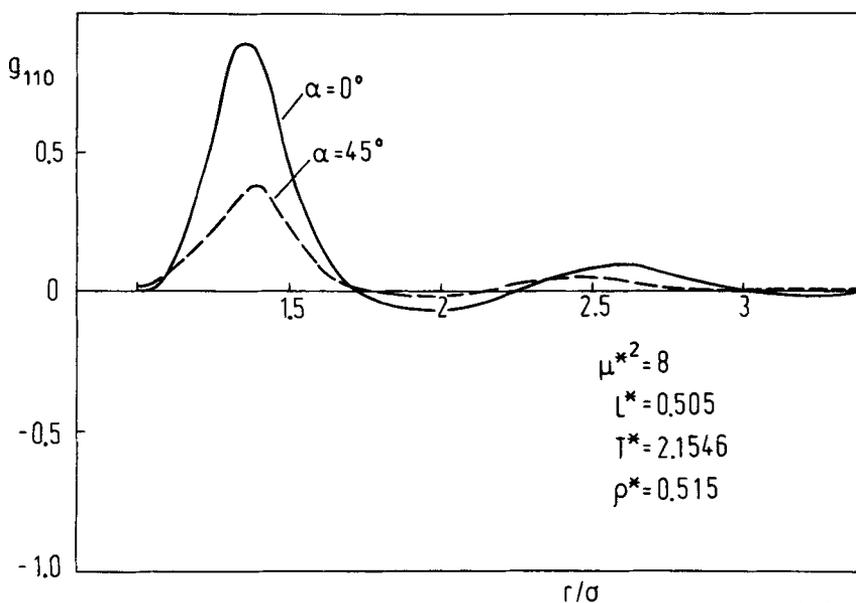
Figure 5. The spherical harmonic expansion coefficients g_{110} of the pair correlation functions of two-centre Lennard-Jones plus dipole fluids for the angles $\alpha = 0°$ and $45°$ between the dipole vector and the molecular axis. For $\alpha = 90°$ this coefficient vanishes.
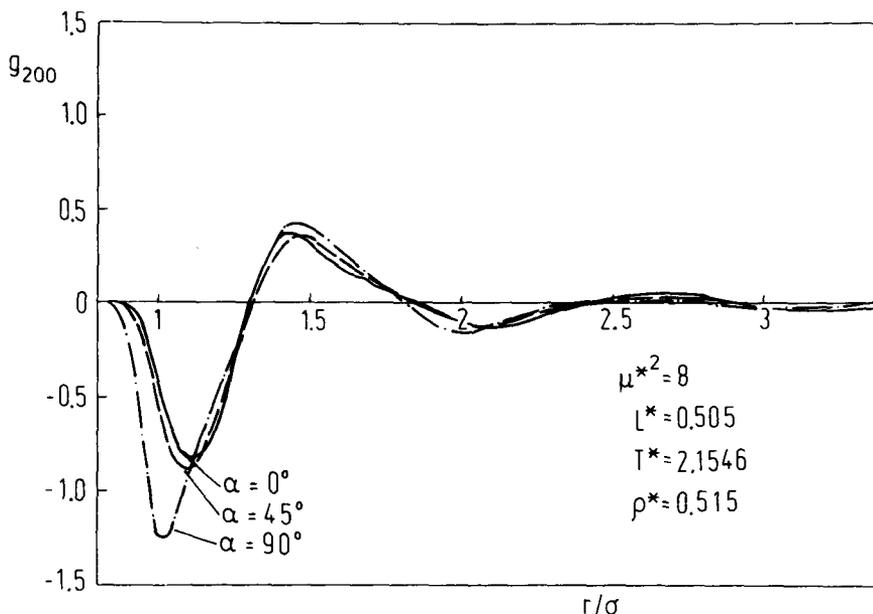
Figure 6. The spherical harmonic expansion coefficients g_{200} of the pair correlation functions of two-centre Lennard-Jones plus dipole fluids for different angles α between the dipole vector and the molecular axis.

centre pair correlation function g_{000} for $\alpha = 90°$ where the first peak is split now into two different peaks. In our opinion the peak at $r = 1·03\sigma$ is connected with the crossed configuration of two molecules which is energetically extremely favourable. For 2CLJ-molecules, the crossed configuration has already the deepest minimum in the energy. Now, if the dipoles form an angle of 90° with the molecular axis, they can in the crossed configuration be in line which is their most favourable mutual orientation, too. Calculating for the crossed configuration the energy as a function of the centre to centre distance, we found the potential minimum at $r = 0·96\sigma$ with $u_{2CLJ-2CLJ} = -1·86\varepsilon$ and $u_{DD} = -18·08\varepsilon$ and hence a total energy value $u_{total} = -19·84\varepsilon$ which is extremely deep compared with the deepest value of -4ε for a simple 2CLJ interaction. As this first peak for $\alpha = 90°$ is very pronounced it seems to be reason for the low pressure and internal energy of this fluid. The deep energy values for the crossed configuration may also be responsible for the negative second virial coefficient.

6. Summary and discussion

Using a simple model, namely the two-centre Lennard-Jones plus dipole along the axis (2CLJD), reasonable predictions can be made for the thermodynamic properties of a non-linear molecule such as CH_3-CHF_2. For most points the calculated pressures agree with the experimental value to within the combined errors. We should note that in the dense liquid the uncertainties of the presently available experiments are of the same order of magnitude as those of the simulations. The energies of vaporization agree with the results of an empirical equation of state within 3 to 8 per cent.

We must, however, admit that for the moment these predictions are not yet as

good as those for the simpler molecules methane [14], oxygen [17], ethane [15, 16, 17], ethylene [17] and propane [18]. The reason for that difference presumably is the fact that the simple molecules were modelled with two or three parameters, whilst for CH_3–CHF_2 a fourth parameter seems to be necessary. The fourth parameter can either be the strength of the dipole moment or, at a given strength, the angle of the dipole vector with the molecular axis. It is obvious that the determination of four parameters is a more difficult problem than that of three. Actually, we were working here only in the space of three parameters as the elongation was fixed from the very beginning. We should also observe that for the simpler molecules the parameters were determined via the saturation curve which we believe to be a very effective method. This has not yet been done but with the newly developed methods for obtaining phase equilibria from simulations [25–27] an improvement can certainly still be achieved in the determination of the parameters.

An other interesting finding was, that the orientation of the dipole has a considerable influence on the thermodynamic and structural properties. With respect to the thermodynamic properties the effect of rotating the dipole out of the axis may be compensated for by a larger dipole moment along the axis.

Note added in proof.—An extensive compilation of thermodynamic and transport property data sets of R152a and R142b was given recently [35].

Appendix

In order to account for the long range interactions of the dipoles in the simulations the reaction field method was used. A very detailed description and investigation of that method will be given elsewhere [32]. The present program is based on a code of Haile [33] who used the quaternion formalism for the rotational equations of motion. Inclusion of the reaction field into that code and vectorization for the CYBER 205 was made by one of us (B.S.). Previous simulations quoted in table 1 were made with 500 particles, all the present runs with 256. The time step in the simulations was $0.0015\sigma(m/\varepsilon)^{1/2}$. Equilibration was performed over 3000 to 8000 time steps and production runs were made with 7000 to 12000 time steps. The cut-off radius was half of the box length and always larger than 3.7σ.

The calculation of the second virial coefficients required three or five fold angular integration. In the three-dimensional case Simpson and Conroy [34] were found to yield identical results, in the five-dimensional case only Conroy's procedure with 3022 orientations was used.

References

[1] Iso, A., and UEMATSU, M., 1989, *Physica* A, **156**, 454.

[2] HIGASHI, Y., ASHIZAWA, M., KABATA, Y., MAJIMA, T., and UEMATSU, M., 1987, *Jap. Soc. Mech. Engrs Int. J.*, **30**, 1106.

[3] SATO, H., UEMATSU, M., and WATANABE, K., 1987, *Fluid Phase Equilib.*, **36**, 167.

[4] FUJIWARA, K., KUBOTA, H., TANAKA, Y., and MAKITA, T., 1986, *Program and Abstracts of the 27th High Pressure Conf. of Japan*, Sapporo, Japan, p. 230.

[5] MAJIMA, T., 1987, M.S. Thesis, supervised by K. Watanabe at Keio University, Yokohama (private communication).

[6] GELLER, V. Z., PORICHANSKI, E. G., SVETLICHNYI, E. G., and ELKIN, Yu. G., 1979, *Kholod. Tekh. Tekhnol.*, **29**, 43.

[7] VALTZ, A., LANGIER, S., and RICHON, D., 1987, *J. chem. Engng Data*, **32**, 397.

[8] SCHRAMM, B., NATOUR, G., and WEBER, CH., Universität Heidelberg (private communication).

[9] MEARS, W. H., STAHL, R. F., ORFEO, S. R., SHAIR, R. C., KELLS, L. F., THOMPSON, W., and McCANN, H., 1955, *Ind. Engng Chem.*, **47**, 1449.

[10] FISCHER, J., LUSTIG, R., BREITENFELDER-MANSKE, H., and LEMMING, W., 1984, *Molec. Phys.*, **52**, 485.

[11] BOHN, M., LUSTIG, R., and FISCHER, J., 1986, *Fluid Phase Equilib.*, **25**, 251.

[12] LUSTIG, R., 1985, *Molec. Phys.*, **59**, 173.

[13] LUSTIG, R., 1987, *Fluid Phase Equilib.*, **32**, 117.

[14] SAAGER, B., and FISCHER, J., *Fluid Phase Equilib.* (in the press).

[15] FISCHER, J., SAAGER, B., BOHN, M., OELSCHLAEGER, H., and HAILE, J. M., 1987, *Molec. Phys.*, **62**, 1175.

[16] LUSTIG, R., TORO-LABBE, A., and STEELE, W. A., 1989, *Fluid Phase Equilib.*, **48**, 1.

[17] SAAGER, B., LOTFI, A., BOHN, M., NGUYEN VAN NHU, and FISCHER, J., 1989, *Fluid Phase Equilib.* (in the press).

[18] LUSTIG, R., and STEELE, W. A., 1988, *Molec. Phys.*, **65**, 475.

[19] BOHN, M., FISCHER, J., and HAILE, J. M., 1988, *Molec. Phys.*, **65**, 797.

[20] SINGER, K., TAYLOR, A., and SINGER, J. V. L., 1977, *Molec. Phys.*, **33**, 1757.

[21] SAAGER, B., and FISCHER, J. (unpublished results).

[22] ASHIZAWA, M., HIGASHI, Y., UEMATSU, M., and WATANABE, K., 1988, *Jap. Soc. Mech. Engrs Int. J.*, **31**, 565.

[23] COSTA CABRAL, B. J., RIVAIL, J. L., and BIGOT, B., 1987, *J. chem. Phys.*, **81**, 1467.

[24] KOHLEN, R., 1987, Dr.-Ing. thesis supervised by F. KOHLER at Ruhr-Universität Bochum. VDI-Verlag, Reihe 19, Nr. 14, Düsseldorf.

[25] PANAGIOTOPOULOS, A. Z., 1987, *Molec. Phys.*, **61**, 813.

[26] GUBBINS, K. E., 1989, *Molec. Simul.*, **2**, 223.

[27] MÖLLER, D., and FISCHER, J., *Molec. Phys.* (submitted).

[28] SWEET, J. R., and STEELE, W. A., 1967, *J. chem. Phys.*, **47**, 3022.

[29] STEINHAUSER, O., 1982, *Molec. Phys.*, **46**, 827.

[30] GIBBS, J. H., and SMYTH, C. P., 1951, *J. Am. chem. Soc.*, **73**, 5115.

[31] GRAY, C. G., and GUBBINS, K. E., 1984, *Theory of Molecular Fluids* (Clarendon Press).

[32] SAAGER, B., FISCHER, J., and NEUMANN, M., manuscript in preparation for submission to *Molec. Simul.* (to be published).

[33] HAILE, J., (private communication).

[34] CONROY, H., 1967, *J. chem. Phys.*, **47**, 5307.

[35] SAAGER, B., and FISCHER, J., 1990, *Tagungdsband der Jahrestagung des Deutschen Kälte- und Klimatechnischen Vereins, Hannover 1989*, edited by A. Grenflo and R. Jakobs (Deutscher Kälte- und Klimatechnischer Verein).